Developments and Applications of Beam & Rod Models

Session Organizer: Carlos LÁZARO (Universidad Politécnica de Valencia)

Keynote Lecture
Finite rotation parameters in statics and in dynamics
Adnan IBRAHIMBEGOVIC (ENS Cachan), Boštjan BRANK (University of Ljubljana)*

An adaptive finite element code using linear Timoshenko beam elements and its applications
Daigoro ISOBE (University of Tsukuba)

The concept of hyper-beams in the analysis of slender members
Salvador MONLEÓN, Fernando IBÁÑEZ, Carlos LÁZARO, Alberto DOMINGO (Universidad Politécnica de Valencia)*

A generalized concept of slenderness in the analysis of straight beams with constant cross-section
Salvador MONLEÓN, Fernando IBÁÑEZ, Alberto DOMINGO, Carlos LÁZARO (Universidad Politécnica de Valencia)*

Element-free solution of geometrically exact rod elastostatics based on intrinsic (material) field variables
Carlos LÁZARO, Salvador MONLEÓN, Alberto DOMINGO (Universidad Politécnica de Valencia)*

Adding local rotational degrees of freedom to ANC beams
Ignacio ROMERO, Juan J. ARRIBAS (Universidad Politécnica de Madrid)*

Finite element modeling of Kirchhoff rods
Juan VALVERDE, Francisco ARMERO (University of California, Berkeley)*

For multiple-author papers:
Contact author designated by *
Presenting author designated by underscore

Proceedings of the 6th International Conference on
Computation of Shell and Spatial Structures
IASS-IACM 2008: "Spanning Nano to Mega"
28-31 May 2008, Cornell University, Ithaca, NY, USA
John F. ABEL and J. Robert COOKE (eds.)

Finite rotation parameters in statics and in dynamics

Adnan IBRAHIMBEGOVIC* and Boštjan BRANK**,

*Ecole Normale Supérieure de Cachan
LMT, 61 av. du president Wilson, 94235 Cachan, France
adnan.ibrahimbegovic@lmt.ens-cachan.fr

** University of Ljubljana, FGG
Jamova 2, 1000 Ljubljana, Slovenia
bbrank@ikpir.fgg.uni-lj.si

Abstract

We examine a number of issues which should be addressed in providing the optimal choice of the finite rotation parameters, both for quasi-statics and dynamics problems. The latter is concerned with the proper choice of rotation parameters, the corresponding update procedure, the symmetry of the tangent operators and the resulting robustness of the solution schemes. The model problems from structural mechanics we consider in detail are beams and shells, both for thin and thick structures, as well as the multibody systems [1,2,3,4,5].

References

[1] Ibrahimbegovic A. W. Schiehlen, Recent advancements in multibody dynamics, Multibody System Dynamics, vol. 8, no. 3, (2002).

[2] Ibrahimbegovic A., W. Kraetzig, Shells: theoretical formulation, mathematical analysis and finite element implementation, Computers and Structures, vol 80, no. 9-10 (2002).

[3] Ibrahimbegovic A. 'On the geometrically exact Formulation of Structural Mechanics and Its Applications to Dynamics, Control and Optimization', Comptes Rendus de l'Academie des Sciences, Part II: Mécanique, 331, 383-394, (2003)

[4] Brank B., S. Mamouri, A. Ibrahimbegovic, 'Constrained finite rotations in dynamics of shells and Newmark implicit time-stepping schemes', International Journal of Engineering Computations, 22, 505-535 (2005)

[5] Ibrahimbegovic A., C. Knopf-Lenoir, A. Kucerova, P. Villon, 'Optimal design and optimal control of elastic structures undergoing finite rotations and deformations', International Joural for Numerical Methods in Engineering, 61, 2428-2460, (2004).

Proceedings of the 6th International Conference on
Computation of Shell and Spatial Structures
IASS-IACM 2008: "Spanning Nano to Mega"
28-31 May 2008, Cornell University, Ithaca, NY, USA
John F. ABEL and J. Robert COOKE (eds.)

An adaptive finite element code using linear Timoshenko beam elements and its applications

Daigoro ISOBE*

* Department of Engineering Mechanics and Energy, University of Tsukuba
1-1-1 Tennodai, Tsukuba-shi, Ibaraki 305-8573, Japan
Email:isobe@kz.tsukuba.ac.jp

Abstract

An adaptive finite element code using linear Timoshenko beam elements called the adaptively shifted integration (ASI) technique and its modified version, the ASI-Gauss technique, have been applied to various numerical simulations on the collapse of framed structures. One of its recent applications was a full model simulation of the aircraft impact with the New York World Trade Center (WTC) Tower 2 in 9/11 terrorist attack in 2001. According to the simulation, springback phenomena due to rapid unloading occurred in the core columns during the impact, which might have caused the destruction of member joints. Another simulation carried out was that of the fire-induced collapse of a high-rise tower mimicking the collapse of WTC 2. The results clearly show the effect of the weak member joints, which were reported to be 20 to 30 % of the strength of the members in WTC towers, and also the effect of the strength reduction due to elevated temperatures.

1. Introduction

An adaptive finite element code called the adaptively shifted integration (ASI) technique was developed by Toi and Isobe [7]. The code can be easily implemented into the existing finite element codes using linear Timoshenko beam elements. In this technique, the numerical integration point is shifted immediately after the occurrence of a fully plastic section in the element so that a plastic hinge is formed exactly at that section. The relationship between the locations of the plastic hinges and the numerical integration points used in the shifting process was first found by Toi [6], and it was obtained by considering the equivalence condition between the strain energy approximation of the finite element and a physical model, the rigid bodies-spring model (RBSM). The technique provided higher computational efficiency than the conventional finite element scheme and was able to cope with dynamic behavior with strong nonlinearities including phenomena such as member fracture. However, it lacked accuracy in the elastic range when the number of elements per member was small due to the low-order displacement function of the linear Timoshenko beam elements. The technique was thus modified into the ASI-Gauss technique (Lynn and Isobe [3]), to improve its accuracy, particularly in the elastic range. The numerical accuracy was increased by placing the numerical integration points of two consecutive elements forming an elastically deformed member in such a way that the stresses and strains are evaluated at the Gaussian integration points of the two-element member, where the accuracy of bending deformation is mathematically guaranteed for two-point integration. This technique gives results with high accuracy at a very low computational cost, even compared with the ASI technique, and is efficient in applications to the dynamic collapse analysis of large-scale framed structures. An outline of the ASI-Gauss technique is described and several numerical simulations on the collapse behaviors of high-rise towers such as the World Trade Center (WTC) towers are discussed in this paper.

2. ASI-Gauss technique

Figure 1 shows a linear Timoshenko beam element and its physical equivalence to the RBSM. As shown in the figure, the relationship between the locations of the numerical integration point and the stress evaluation point where a plastic hinge is formed is expressed as (Toi [6])

$$r = As \tag{1}$$

In the above equation, *s* is the location of the numerical integration point and *r* is the location where stresses and strains are evaluated. *s* and *r* are nondimensional quantities that take values between -1 and 1.

In both the ASI and ASI-Gauss techniques, the numerical integration point is shifted adaptively when a fully plastic section is formed within an element to form a plastic hinge exactly at that section. When the plastic hinge is unloaded, the corresponding numerical integration point is shifted back to its normal position. Here, the normal position means the location where the numerical integration point is placed when the element acts elastically. By doing so, the plastic behavior of the element is simulated appropriately, and the converged solution is achieved with only a small number of elements per member. However, in the ASI technique, the numerical integration point is placed at the midpoint of the linear Timoshenko beam element, which is considered to be optimal for one-point integration, when the entire region of the element behaves elastically. When the number of elements per member is very small, solutions in the elastic range are not accurate since one-point integration is used to evaluate the low-order displacement function of the beam element.

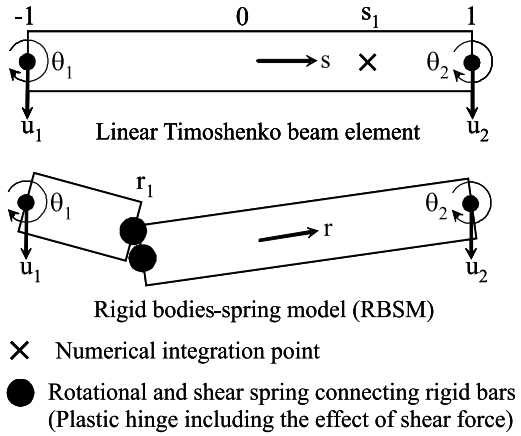

Figure 1: Linear Timoshenko beam element and its physical equivalent

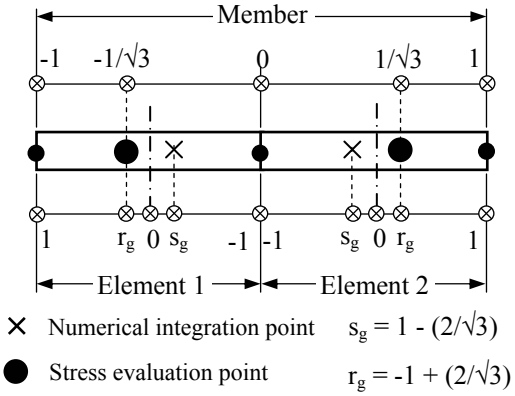

Figure 2: Locations of numerical integration and stress evaluation points in ASI-Gauss technique

The main difference between the ASI and ASI-Gauss techniques lies in the normal position of the numerical integration point. In the ASI-Gauss technique, two consecutive elements forming a member are considered as a subset, as shown in Fig. 2, and the numerical integration points of an elastically deformed member are placed such that the stress evaluation points coincide with the Gaussian integration points of the member. This means that stresses and strains are evaluated at the Gaussian integration points of elastically deformed members. Gaussian integration points are optimal for two-point integration and the accuracy of bending deformation is mathematically guaranteed (Press *et al.* [5]). In this way, the ASI-Gauss technique takes advantage of two-point integration while using one-point integration in actual calculations.

Structurally discontinuous problems also become easily handled using the ASI and ASI-Gauss techniques by shifting the numerical integration point of the linear Timoshenko beam element to an appropriate position and by releasing the resultant forces in the element simultaneously. Axial tensile strain, shear strains and bending strains are used for the fracture criterion. Elemental contact is considered in the code by introducing gap elements between pairs of elements determined to be in contact by geometrical relations. More details on the code can be found in Lynn and Isobe [3] and Isobe and Sasaki [2].

3. Numerical examples

3.1 Analysis of aircraft impact with the World Trade Center tower

We performed an analysis of the aircraft impact with a full-scale model of WTC Tower 2 (Isobe and Sasaki [2]) using the code described in the previous section. Details on the structural members and construction data are extracted and adopted from previous reports (ASCE/FEMA [1] and NIST [4]). The tower and the B767-200ER aircraft are both modeled using linear Timoshenko beam elements, of which all members are subdivided into

two elements. The tower model contains 604,780 elements, 435,117 nodes and 2,608,686 degrees of freedom, while the aircraft model contains 4,322 elements, 2,970 nodes and 17,820 degrees of freedom. The total mass of the aircraft at the time of impact is 142.5 t, which is the sum of the masses of the aircraft (112.5 t) and the jet fuel (30 t). The mass of each engine is assumed to be 19.315 t. The nose of the aircraft is tilted 11.5 degrees to the east and 5 degrees downward, and its left wing is inclined downward by 35 degrees. It is assumed to collide with the 81st floor on the south face of WTC 2 with a cruising speed of 590 mph (262 m/s).

(a) 0.12 s, (b) 0.28 s and (c) 0.56 s after impact
Figure 3: Analysis of aircraft impact with WTC 2 (global view)

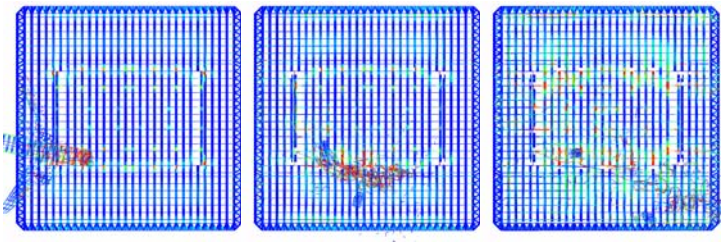

(a) 0.12 s, (b) 0.28 s and (c) 0.56 s after impact
Figure 4: Motion of fuselage and engines (upper view)

The numerical results are shown in Figs. 3 and 4. The left engine reduces its speed rapidly as it directly enters the core structure. The right engine, on the other hand, glances off the core structure and passes through the north-east corner of the tower. Figure 5 shows the transition of axial forces in a typical core column every ten stories from the ground floor to the top floor. The core column is compressed constantly until the front of the plane reaches the core structure (Phase A in the figure), after which a wave due to the impact and member fracture propagates in the horizontal and vertical directions. In particular, the compression decreases instantaneously in the fractured core column (No. 1001) at the floors above the impact point. At the lower levels, compression changes to tension immediately after the left engine hits the core structure (Phase C), and the values of axial forces continue to vibrate with large amplitude. Note that the lower the height, the larger the amplitude becomes. The core column (No.1001) at the 60th floor, for example, moves vertically for 25 cm in 0.2 s as a result of this dynamic transition.

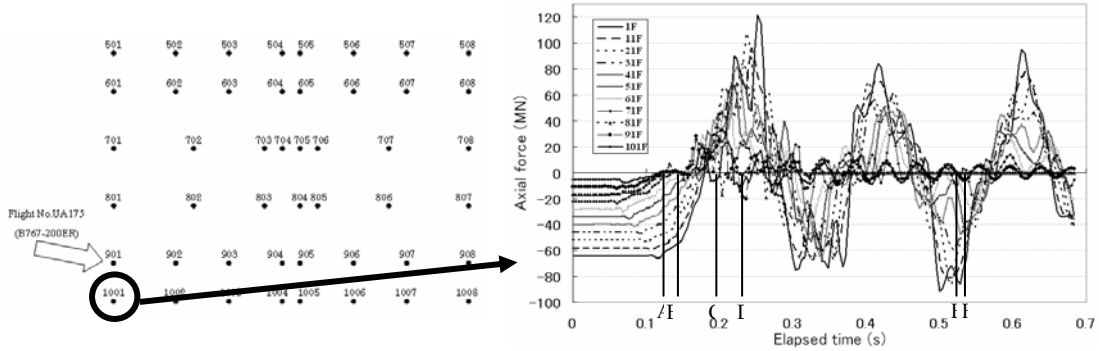

Figure 5: Time histories of axial forces in core column No.1001

3.2 Analysis of fire-induced collapse of high-rise towers

The analysis of fire-induced collapse is carried out on a 25-story 3-span tower to determine the effect of the strength reduction due to elevated temperatures. Two cases are analyzed: a strong-member-joint model (member

joints with 100 % strength compared with the member strength) and a weak-member-joint model (member joints with 20 % strength), on the basis of the fact that the member joint strengths of typical core columns were about 20 to 30 % of those of the members in the WTC towers (ASCE/FEMA [1]). Curves showing the reduced modulus of elasticity and yield strength due to elevated temperatures (NIST [4]) are adopted. It has been reported that the modulus of elasticity of the columns is reduced to 60 % of the original value, and the yield strength to 10 % of the original strength, at 700 □. We can clearly see the difference between the two models in Fig. 6 when the three middle blocks of the 17th to 19th floors are heated to 700 □. A red color means that a plastic hinge is formed within the element. Fractured elements are painted out with white color. The strong-member-joint model withstands the elevated temperature by redistributing the stresses in the tower while the weak-member-joint model starts to collapse once it buckles at the floors that are on fire.

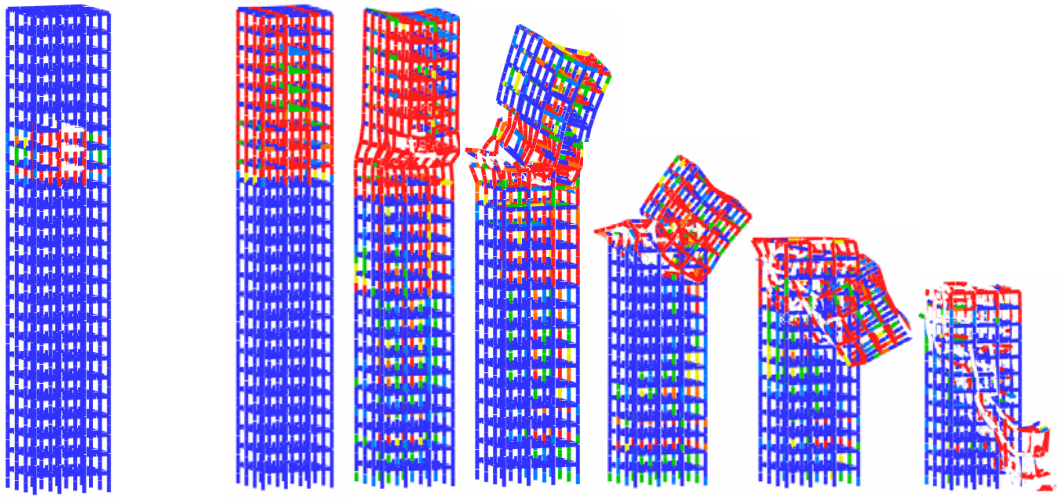

(a) Strong-member-joint model (final phase) (b) Weak-member-joint model (progressive collapse sequence)

Figure 6: Analysis of fire-induced collapse of a high-rise tower

4. Conclusion

The adaptive finite element code using linear Timoshenko beam elements described in this paper can be applied to various collapse problems of framed structures. Other examples of analyses on blast demolition and seismic collapse are to be presented at the conference.

References

[1] ASCE/FEMA. World Trade Center Building Performance Study: Data Collection, Preliminary Observation and Recommendations, 2002.

[2] Isobe D and Sasaki Z. Aircraft Impact Analyses of the World Trade Center Towers, *CD-ROM Proceedings of the 1st International Workshop on Performance, Protection, and Strengthening of Structures under Extreme Loading (PROTECT2007)*, Whistler, Canada, 2007.

[3] Lynn KM and Isobe D. Finite Element Code for Impact Collapse Problems of Framed Structures, *International Journal for Numerical Methods in Engineering* 2007; **69(12)**: 2538-2563.

[4] NIST NCSTAR 1. Federal Building and Fire Safety Investigation of the World Trade Center Disaster: Final Report on the Collapse of the World Trade Center Towers, National Institute of Standards and Technology (NIST), 2005.

[5] Press WH, Teukolsky SA, Vetterling WT and Flannery BP. Numerical Recipes in FORTRAN: The Art of Scientific Computing, New York: Cambridge University Press, 1992.

[6] Toi Y. Shifted Integration Technique in One-Dimensional Plastic Collapse Analysis Using Linear and Cubic Finite Elements, *International Journal for Numerical Methods in Engineering* 1991; **31**: 1537-1552.

[7] Toi Y and Isobe D. Adaptively Shifted Integration Technique for Finite Element Collapse Analysis of Framed Structures, *International Journal for Numerical Methods in Engineering* 1993; **36**: 2323-2339.

Proceedings of the 6th International Conference on
Computation of Shell and Spatial Structures
IASS-IACM 2008: "Spanning Nano to Mega"
28-31 May 2008, Cornell University, Ithaca, NY, USA
John F. ABEL and J. Robert COOKE (eds.)

The concept of hyper-beams in the analysis of slender members

Salvador MONLEÓN*, Fernando IBÁÑEZ, Carlos LÁZARO, Alberto DOMINGO

*Departamento de Mecánica de Medios Continuos y Teoría de Estructuras
ETS Ingenieros de Caminos, Universidad Politécnica de Valencia
smonleon@mes.upv.es

Abstract

All problems of the theory of beams are formulated in an identical manner when we decide to use variational analysis. Within the scope of the static of elastic beams, if $F(s,\mathbf{u},\mathbf{u}')$ is the functional of the problem, $\mathbf{u}$(s) the generalized displacements and s the arc-length along the curved axis of the element, the Euler-Lagrange equations systematically provide us with the ordinary differential equations of the problem. These constitute a convenient frame to develop a unified formulation of the analysis of slender members. We will use the Legendre's transformation to improve the deduction of the system of differential equations governing the problem and to define the linear density of complementary energy of the 1D model. We will finally deal with the explicit determination of the components of the operators that form the theory and their values at the specific case of the standard beam (Navier-Bernoulli-Timoshenko). The results will allow us to deduce the conditions on which the elementary problems get uncoupled as well as to introduce and justify the new concept of hyper-beam.

1. Legendre's transformation

Legendre's transformation (Lanczos [1]) provides us with an elegant way to obtain the canonical form of the equations of the problem. To do so we will introduce a new function $H(s,\mathbf{u},\mathbf{f})$ by means of the equation:

$$H = \mathbf{f}^T\left(\mathbf{H}^T\mathbf{u} + \mathbf{u}'\right) - F$$

being $\mathbf{H} = \mathbf{D}_{01}\mathbf{D}_{11}^{-1}$ the local equilibrium matrix (Monleón [3]). Solving the equation of definition of generalised stresses in $\mathbf{u}'$ and substituting it in the expression of the linear density of potential energy F of the model, we can find the desired form of the function $H(s,\mathbf{u},\mathbf{f})$. In the linear case, this means:

$$\mathbf{f} = \frac{\partial F}{\partial \mathbf{u}'} = \mathbf{D}_{10}\mathbf{u} + \mathbf{D}_{11}\mathbf{u}'$$

so $\mathbf{u}' = \mathbf{D}_{11}^{-1}\left(\mathbf{f} - \mathbf{D}_{10}\mathbf{u}\right) = \mathbf{D}_{11}^{-1}\mathbf{f} - \mathbf{H}^T\mathbf{u}$ and $H = \frac{1}{2}\left(\mathbf{f}^T\mathbf{D}_{11}^{-1}\mathbf{f} - \mathbf{u}^T\hat{\mathbf{D}}_{00}\mathbf{u}\right) + \mathbf{u}^T\mathbf{Q}$, being $\hat{\mathbf{D}}_{00} = \mathbf{D}_{00} - \mathbf{D}_{01}\mathbf{D}_{11}^{-1}\mathbf{D}_{10}$.
Considering that the definitions of H and F require:

$$\frac{\partial H}{\partial \mathbf{f}} = \mathbf{H}^T\mathbf{u} + \mathbf{u}', \quad \frac{\partial H}{\partial \mathbf{u}} = \mathbf{H}\mathbf{f} - \frac{\partial F}{\partial \mathbf{u}} = \mathbf{H}\mathbf{f} - \mathbf{f}'$$

The equations of the problem are thus transformed into:

$$\mathbf{u}' = \frac{\partial H}{\partial \mathbf{f}} - \mathbf{H}^T\mathbf{u} = \mathbf{D}_{11}^{-1}\mathbf{f} - \mathbf{H}^T\mathbf{u}, \quad \mathbf{f}' = \mathbf{H}\mathbf{f} - \frac{\partial H}{\partial \mathbf{u}} = \mathbf{H}\mathbf{f} + \hat{\mathbf{D}}_{00}\mathbf{u} - \mathbf{Q}$$

When we arrange them in a matrix form:

$$\begin{Bmatrix}\mathbf{u}' \\ \mathbf{f}'\end{Bmatrix} = \begin{bmatrix}-\mathbf{H}^T & \mathbf{D}_{11}^{-1} \\ \hat{\mathbf{D}}_{00} & \mathbf{H}\end{bmatrix}\begin{Bmatrix}\mathbf{u} \\ \mathbf{f}\end{Bmatrix} - \begin{Bmatrix}\mathbf{0} \\ \mathbf{Q}\end{Bmatrix}$$

As a result the function $H(s,\mathbf{u},\mathbf{f})$ directly provides the canonical form of the equations of the equilibrium problem. Let us note that the definition of H adopted herein is slightly different than the traditional one[1]: $H = \mathbf{f}^T\mathbf{u}' - F$. Nevertheless $H(s,\mathbf{u},\mathbf{f})$ being referenced to the generalised strains $\mathbf{e} = \mathbf{H}^T\mathbf{u} + \mathbf{u}'$, it

corresponds to the *linear density of complementary energy* of the model (see Table I). In resume, Legendre's transformation has provided with the next dual structures (Lanczos [1]):

	Original system	**New system**
Function	Lagrangian $F(s,\mathbf{u},\mathbf{u}')$ linear density of potential energy	Hamiltonian $H(s,\mathbf{u},\mathbf{f})$ linear density of complementary energy
Variables	Generalised strains $\mathbf{e}(s)$	Generalised stresses $\mathbf{f}(s)$
Duality	$\dfrac{\partial F}{\partial \mathbf{e}} = \mathbf{f}$	$\dfrac{\partial H}{\partial \mathbf{f}} = \mathbf{e}$
(linear case)	$H = \mathbf{f}^T\mathbf{e} - F$ $F = \frac{1}{2}\left(\mathbf{e}^T\mathbf{D}_{11}\mathbf{e} + \mathbf{u}^T\hat{\mathbf{D}}_{00}\mathbf{u}\right) - \mathbf{u}^T\mathbf{Q}$	$F = \mathbf{f}^T\mathbf{e} - H$ $H = \frac{1}{2}\left(\mathbf{f}^T\mathbf{D}_{11}^{-1}\mathbf{f} - \mathbf{u}^T\hat{\mathbf{D}}_{00}\mathbf{u}\right) + \mathbf{u}^T\mathbf{Q}$
Equilibrium equations	$\dfrac{\partial F}{\partial \mathbf{u}} = \mathbf{f}'$	$\dfrac{\partial H}{\partial \mathbf{u}} = \mathbf{H}\mathbf{f} - \mathbf{f}'$

Table 1. Resume of Legendre's transformation

2. Unified formulation's characteristics operators

2.1. Solid's geometry.

$\mathbf{P}(s,y,z) = \mathbf{R}(s) + y\mathbf{n}(s) + z\mathbf{b}(s)$, $\mathbf{R}$ is the position vector of the points of Γ and L is the length of the element, whereas the cross-section A can vary along it.

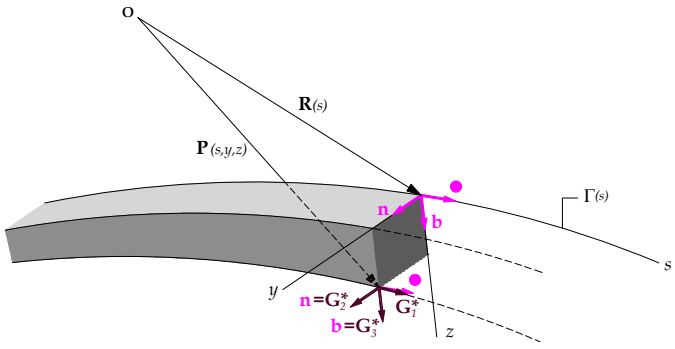

Figure 1. *Graphical definition of the coordinated lines and surfaces of the system (s,y,z)*

The following formula resumes the condition of slender member: $h/L \le \varepsilon$, $h = \sqrt{(y_{\max} - y_{\min})^2 + (z_{\max} - z_{\min})^2}$, where h is the maximum height of the cross-section and ε<<1. The natural vectors of the above defined curvilinear coordinates system are:

$$\mathbf{G}_1^* = \frac{\partial \mathbf{P}}{\partial s} = \mu\boldsymbol{\lambda} - \tau(z\mathbf{n} - y\mathbf{b}), \quad \mathbf{G}_2^* = \frac{\partial \mathbf{P}}{\partial y} = \mathbf{n}, \quad \mathbf{G}_3^* = \frac{\partial \mathbf{P}}{\partial z} = \mathbf{b}$$

with μ=1−χy, being χ the curvature and τ the torsión of the curved axis $\Gamma(s)$.

2.2. Deformed configuration.

The position of the material points of B and the natural vectors associated to the new configuration become:

$$\mathbf{p}(s,y,z) = \mathbf{P}(s,y,z) + \mathbf{d}^*(s,y,z)$$

and

$$\mathbf{g}_1^* = \frac{\partial \mathbf{p}}{\partial s} = \mathbf{G}_1^* + \frac{\partial \mathbf{d}^*}{\partial s} + \boldsymbol{\Omega}_0^T\mathbf{d}^*, \quad \mathbf{g}_2^* = \frac{\partial \mathbf{p}}{\partial y} = \mathbf{n} + \frac{\partial \mathbf{d}^*}{\partial y}, \quad \mathbf{g}_3^* = \frac{\partial \mathbf{p}}{\partial z} = \mathbf{b} + \frac{\partial \mathbf{d}^*}{\partial z}$$

Where $\mathbf{\Omega}_0$ defines the evolution of the Frênet-Serret trihedron along the curved axis and vector $\mathbf{d}^*(s,y,z)$ states for the displacement of the points $\mathbf{P}(s,y,z)$ due to the change of configuration.

2.3. Physical components of the infinitesimal strains.

These components can be written in the form of linear differential operators (Monleón [3]):

$$\mathbf{e}^* = \left\{\varepsilon_s^* \quad \varepsilon_y^* \quad \varepsilon_z^* \quad \gamma_{sy}^* \quad \gamma_{sz}^* \quad \gamma_{yz}^*\right\}^T = \left[\mathbf{E}_1 \frac{\partial}{\partial s} + \mathbf{E}_2 \frac{\partial}{\partial y} + \mathbf{E}_3 \frac{\partial}{\partial z} - \mathbf{E}_1\mathbf{\Omega}_0\right].\mathbf{d}^*$$

being $\gamma^* = 1 + (\tau/\mu)^2\left(y^2 + z^2\right)$. Let us apply now the fundamental hypothesis and thus: $\mathbf{e}^* = \mathbf{B}_0\mathbf{u} + \mathbf{B}_1\mathbf{u}'$, with the deformation matrixes: $\mathbf{B}_0 = \mathbf{E}_2\mathbf{h}_{,y} + \mathbf{E}_3\mathbf{h}_{,z} - \mathbf{E}_1\mathbf{\Omega}_0\mathbf{h}$, $\mathbf{B}_1 = \mathbf{E}_1\mathbf{h}$.

3. The "Standard Beam" model

In such model, the fundamental hypothesis (Monleón [3]) corresponds to an infinitesimal rigid body displacement:

$$\mathbf{d}^*(s,y,z) = \begin{bmatrix}\mathbf{I} & \mathbf{\Lambda}\end{bmatrix}\begin{Bmatrix}\mathbf{d}\\ \boldsymbol{\theta}\end{Bmatrix}, \quad \mathbf{\Lambda} = \begin{bmatrix} 0 & z & -y \\ -z & 0 & 0 \\ y & 0 & 0 \end{bmatrix}$$

$\mathbf{d}=\{u\ v\ w\}^T$ defines the translation of the section and $\boldsymbol{\theta}=\{\theta_s\ \theta_y\ \theta_z\}^T$ their infinitesimal rotations with respect to the coordinated lines. The strain energy is determined by the matrixes:

$$\mathbf{D}_{00} = \int_A \mathbf{B}_0^T\mathbf{C}\mathbf{B}_0\mu dA, \quad \mathbf{D}_{01} = \int_A \mathbf{B}_0^T\mathbf{C}\mathbf{B}_1\mu dA, \quad \mathbf{D}_{11} = \int_A \mathbf{B}_1^T\mathbf{C}\mathbf{B}_1\mu dA$$

Evaluating $\mathbf{D}_{01}\mathbf{D}_{11}^{-1}\mathbf{D}_{10}$ and considering the particular composition of $\mathbf{h}(s,y,z)$, it can be checked that the standard beam model, or the *beam model* in a simpler way (the cross-sections can only have an infinitesimal rigid body displacement), possesses the following characteristic: $\hat{\mathbf{D}}_{00} = \mathbf{D}_{00} - \mathbf{D}_{01}\mathbf{D}_{11}^{-1}\mathbf{D}_{10} = \mathbf{0}$. This is independent of the shape of the axis curve *Γ(s)*.

4. Uncoupling of the static problem and "hyper-beams"

Proposition 1*. It is* ***necessary*** *that the deformation matrixes satisfy a relationship of the form* $\hat{\mathbf{D}}_{00} = \mathbf{D}_{00} - \mathbf{D}_{01}\mathbf{D}_{11}^{-1}\mathbf{D}_{10} = \mathbf{0}$ *so that the equations of equilibrium of the 1D model can adopt a purely static expression (uncoupling of the equilibrium), i.e. they can be expressed as a linear combination of the vector* $\mathbf{f}(s)$ *and its derivative.*

Making use of the linear density of complementary energy we obtain directly: $\frac{\partial H}{\partial \mathbf{u}} = \mathbf{H}\mathbf{f} - \mathbf{f}' = \mathbf{Q} - \hat{\mathbf{D}}_{00}\mathbf{u}$.

Consequently, this equation will only adopt a pure static expression if $\mathbf{D}_{00} = \mathbf{H}\mathbf{D}_{11}\mathbf{H}^T$ ■

Proposition 2. *It is* ***sufficient*** *that the fundamental hypothesis of the 1D model represents a rigid body displacement of the cross-section so that the equations of equilibrium of the 1D model can adopt an expression purely static (uncoupling of the equilibrium), i.e. they can be expressed as a linear combination of the vector* $\mathbf{f}(s)$ *and its derivative.*

Let us base on the fundamental hypothesis defined: in this case the components of the vector of generalised stresses are directly:

$$\mathbf{f}(s) = \int_A \mathbf{h}^T\mathbf{t}^* dA = \int_A \begin{bmatrix}\mathbf{I}\\ \mathbf{\Lambda}^T\end{bmatrix}\mathbf{t}^* dA = \begin{Bmatrix}\mathbf{N}(s)\\ \mathbf{M}(s)\end{Bmatrix}$$

being the vectors $\mathbf{N} = \int_A \mathbf{t}^*\, dA$, $\mathbf{M} = \int_A \mathbf{\Lambda}^T\mathbf{t}^*\, dA$, which three components are defined as the typical stresses: axial and shear forces, torque and bending moments respectively. Let us define $\mathbf{Q}_N$ and $\mathbf{Q}_M$ as the linear

densities of force and moment applied to the model. The linear *vectorial* equilibrium of the element requires that the following equilibrium equations are accomplished (Figure 2):

$$\mathbf{N}' - \mathbf{\Omega}_0\mathbf{N} + \mathbf{Q}_N = \mathbf{0}, \quad \mathbf{M}' - \mathbf{\Omega}_0\mathbf{M} + \boldsymbol{\lambda}\times\mathbf{N} + \mathbf{Q}_M = \mathbf{0}$$

But $\boldsymbol{\lambda}\times\mathbf{N} \equiv \mathbf{\Lambda}_0\mathbf{N}$ and thus we finally obtain $\mathbf{f}' - \mathbf{H}\mathbf{f} + \mathbf{Q} = \mathbf{0}$. *Six* equations in the *six* components of the generalised stresses **f**(*s*) are sufficient to determine the equilibrium. Those are consistent with the fundamental hypothesis adopted: an infinitesimal rigid body displacement of the cross-section of the slender member■

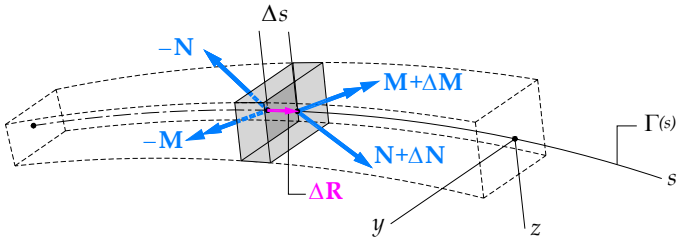

Figure 2. *Generalised stresses at the vectorial equilibrium of the beam*

Within the scope of the 1D analysis of slender members, we will refer to the hyper-beam model when the following conditions are satisfied:

(1) ***Necessary condition****. The fundamental hypothesis includes at least one component of displacement different than the infinitesimal rigid body displacement of the cross-section.*

(2) ***Sufficient condition****. The equilibrium equations couple stresses and displacements, and thus*

2.1 At the general case (non linear problems) this requires:

$$\frac{\partial^2 H}{\partial \mathbf{u}^2} \neq \mathbf{0}$$

2.2 In the linear case it is sufficient to verify $\hat{\mathbf{D}}_{00} = \mathbf{D}_{00} - \mathbf{H}\mathbf{D}_{11}\mathbf{H}^T \neq \mathbf{0}$ ■

5. Conclusions

1. We systematically introduced at the formulation the local equilibrium matrix of the model **H**, equal to $\mathbf{D}_{01}\mathbf{D}_{11}^{-1}$ in the general case.
2. We adopted new measures of the strains at the model by defining the *generalised strains* as $\mathbf{e} = \mathbf{H}^T\mathbf{u} + \mathbf{u}'$. Legendre's transformation allowed us to obtain its *linear density of complementary energy*:
$$H(s,\mathbf{u},\mathbf{f}) = \tfrac{1}{2}\left(\mathbf{f}^T\mathbf{D}_{11}^{-1}\mathbf{f} - \mathbf{u}^T\hat{\mathbf{D}}_{00}\mathbf{u}\right) + \mathbf{u}^T\mathbf{Q}\,.$$
We also re-wrote the *linear density of potential energy* (Washizu [2]) as $F = \tfrac{1}{2}\left(\mathbf{e}^T\mathbf{D}_{11}\mathbf{e} + \mathbf{u}^T\hat{\mathbf{D}}_{00}\mathbf{u}\right) - \mathbf{u}^T\mathbf{Q}$, pointing out the complementary character of both functions as well as the dualities established at Table I.
3. We demonstrated that it is not always possible to find a pure static form of the equilibrium equations
4. Based on this idea we built the conditions proposed for the definition of the *hyper-beams*. We can note as examples the torsion (Vlassov [5]) and distortion theories, including the anti-clastic bending (Oden *et al.* [4]), or any bending theory using warping patterns other than the linear one.

References

[1] Lanczos, C., The Variational Principles of Mechanics, University of Toronto Press, 4th ed. (1970), Dover (1986)
[2] Washizu, K., Variational Methods in Elasticity and Plasticity, Pergamon Press, 2nd ed. (1974)
[3] Monleón, S., Análisis de Vigas, Arcos, Placas y Láminas: una presentación unificada, 2nd ed., Editorial UPV, Ref. 2001.4122 (2001)
[4] Oden, J.T. and Ripperger, E.A., Mechanics of Elastic Structures, Mc Graw-Hill, 2nd ed. (1981)
[5] Vlassov, B.Z., Pièces Longues en Voiles Minces, Eyrolles Editeurs, 2nd ed. (1962)

Proceedings of the 6th International Conference on
Computation of Shell and Spatial Structures
IASS-IACM 2008: "Spanning Nano to Mega"
28-31 May 2008, Cornell University, Ithaca, NY, USA
John F. ABEL and J. Robert COOKE (eds.)

A Generalized Concept Of Slenderness In The Analysis Of Straight Beams With Constant Cross-Section

Salvador MONLEÓN*, Fernando IBÁÑEZ, Alberto DOMINGO, Carlos LÁZARO

* ETS Ingenieros de Caminos, Universidad Politécnica de Valencia
Camino de Vera s/n, 46022 Valencia
smonleon@mes.upv.es

Abstract

The existence of analogies between all beam elastostatic problems appears because they can be formulated using the same procedure: if $F(s,\mathbf{u},\mathbf{u}')$ is the linear density of potential energy, $\mathbf{u}(s)$ are the generalized displacements, and s is the arc-length parameter along the curved axis of the member, then the variational equation (Benscoter [1], Maisel [8])

$$\frac{\partial F}{\partial \mathbf{u}} - \frac{d}{ds}\left(\frac{\partial F}{\partial \mathbf{u}'}\right) = \mathbf{0} \tag{1}$$

systematically provides the ordinary differential field equations of the problem. For beams with constant curvature and cross-section, the system of differential equations has constant coefficients. In this case the solution depends on the system-matrix eigenvalues, which can be presented as *slenderness* by normalizing the arc-length parameter s. Thus, it can be stated that the behavior or nature of the response of each 1D problem is determined by the value of the corresponding slenderness. We will base our work in four uncoupled elementary problems to consolidate this statement. We will start by reviewing the main concepts necessary to apply the *unified formulation* for the analysis of slender members already presented in previous works (Kollbrunner & Basler [5]) and used herein as the calculation tool. Subsequently we will introduce a new definition of the mechanical concept of *slenderness* for the 1-D model of straight beams with constant cross-section and we will show how this parameter fully controls the member response. This will allow us to demonstrate interesting conclusions regarding the properties of the solutions, the classification of beams for modeling, and also about the generalization of physical analogies.

1. Results obtained in four uncoupled problems

By using the explicit form of the $F(s,\mathbf{u},\mathbf{u}')$ function (Monleón [9], [11]), the system of differential equations that governs the problem can be written in the form:

$$\frac{d}{ds}\mathbf{E}(s) = \mathbf{W}.\mathbf{E}(s) - \mathbf{F}(s) \tag{2}$$

At the equation (2), $\mathbf{E}(s)$ is the state vector that contains all the variables of the problem (generalised displacements and efforts) and $\mathbf{F}(s)$ is the vector of independent terms or vector of loads:

$$\mathbf{E}(s) = \begin{Bmatrix} \mathbf{u}(s) \\ \mathbf{f}(s) \end{Bmatrix} \qquad \mathbf{F}(s) = \begin{Bmatrix} \mathbf{0} \\ \mathbf{Q}(s) \end{Bmatrix} \tag{3}$$

The operator $\mathbf{W}$ is a function of the generalised local stiffness $\mathbf{D_{rs}}$ (Monleón [11]) that derive directly from the fundamental hypothesis of displacements and the cross-section geometry:

$$\mathbf{W} = \begin{bmatrix} -\mathbf{D}_{11}^{-1}\mathbf{D}_{10} & \mathbf{D}_{11}^{-1} \\ \mathbf{D}_{00} - \mathbf{D}_{01}\mathbf{D}_{11}^{-1}\mathbf{D}_{10} & \mathbf{D}_{01}\mathbf{D}_{11}^{-1} \end{bmatrix} \tag{4}$$

In problems relative to straight beams with constant cross-section **W** is a constant matrix and its eigenvalues K are defined by means of the characteristic equation:

$$\left|\mathbf{W} - K\mathbf{I}\right| = 0 \tag{5}$$

The solution is built by linearly combining functions of the type $e^{Ks}\mathbf{E}_K \equiv e^{\lambda\xi}\mathbf{E}_K$ where $\mathbf{E}_K$ is the eigenvector associated to the eigenvalue K, $\xi=s/L$ is the normalised length of arc at the axis and $\lambda=KL$ is a non-dimensional parameter. The λ parameter is key to the nature of the solution: it is at the base of the discussion of the characteristic solutions and controls the extent to which each phenomenon is influential, in particular the generalised displacements.

Let us now consider four classic problems of the beam's theory that will be studied as uncoupled. We present them by means of their associated linear density of potential energy and then resume in a table the parameters controlling each response.

I(a) Mixed torsion: The theory of torsion of beams presented therein rests on the assumption that the warp displacements are proportional to the unitary torsion rotation (Vlassov [15] and Kollbrunner & Basler [5]). Its main property is to allow for the connection two different theories: the warped torsion at elements of thin wall cross-section and Pure torsion of St Venant [14]. Assuming that the density of warp φ(x) and the torsion rotation $\theta_x(x)$ are independent functions (Oden [12] & Oumanski [13], i.e. that $\varphi(x) \neq \theta_x'(x)$, a slightly different solution (Benscoster [1], Manterola [7] & Monleón [10]) to this problem can be found. In this problem the linear density of potential energy can be expressed as:

$$F = \tfrac{1}{2}\left[GJ(\theta_x')^2 + GW_C(\theta_x' - \varphi)^2 + EI_{\hat{\omega}}(\varphi')^2\right] - \left(m_x\theta_x + b_{\hat{\omega}}\varphi\right) \tag{6}$$

where m_x and b_w are the loads (torques and bi-moments), and the static constants of polar moment of inertia $\Im_C$ and modulus of warping $I_{\hat{\omega}}$ ($W_C = \Im_C - J$, with J being the module of torsion of the cross-section).

I(b) Column beam (Brush [2]): A linear element subjected to axial compression and transverse loading is conventionally named *column beam*. We study its behaviour in the field of geometrical non-linearity, both for tension or compression axial force. In such case, the linear density of potential energy that derives is:

$$F = \tfrac{1}{2}\left\{EA\left[u' + \tfrac{1}{2}(v')^2\right]^2 + GA(v' - \theta_z)^2 + EI_z(\theta_z')^2\right\} - \left(q_y v + m_z\theta_z\right) \tag{7}$$

where q_y and m_z are the well-known transverse loads and moments, A the cross-section and I_z the moment of inertia. Finally, $N_0 = EA\left[u' + \tfrac{1}{2}(v')^2\right]$ is the force applied to both ends of the model in the direction of the longitudinal axis, that is acting here as a known constant, positive in tension.

II(a) Distortion (Dabrowski [3], Kristek [6], Manterola [7] & Monleón [9]): this problem is typical of the beams of thin walled cross-section and allows us to disregard one of the main hypothesis of the standard theory of beams (non deformable transverse section). Nevertheless, in the case of hollow box cross-sections a 1-D formulation of distortion can be built when shear lag is negligible. If m_D and b_D define the linear densities of load, in this case distortion "bi-shears" and distortion bi-moments, and GW_D and EI_D are the membrane stiffness of the element and EI_b the frame stiffness of the beam, the linear density of potential energy is shown next:

$$F = \tfrac{1}{2}\left[EI_b\gamma_D^2 + GW_D(\gamma_D' - \varphi_D)^2 + EI_D(\varphi_D')^2\right] - \left(m_D\gamma_D + b_D\varphi_D\right) \tag{8}$$

II(b) Floating beam (Hetenyi [4]): this corresponds to the soil model of Winkler, extended through the work of Zimmermann for the analysis of rails upon sleepers of railroads. Being k the so called *ballast coefficient,* the linear density of potential energy becomes in this case:

$$F = \tfrac{1}{2}\left[kv^2 + GA(v' - \theta_z)^2 + EI_z(\theta_z')^2\right] - \left(q_y v + m_z\theta_z\right) \tag{9}$$

The generalised local stiffness, eigenvalues and associated slenderness are resumed at the next table.

PROBLEM	D	eigenvalues K	slenderness λ	Additional factors
TORSION	$\begin{bmatrix} 0 & 0 & 0 & 0 \\ 0 & GW_C & -GW_C & 0 \\ 0 & -GW_C & G\Im_C & 0 \\ 0 & 0 & 0 & EI_\omega \end{bmatrix}$	$K^2=0; K^2=\left(\frac{\lambda_T}{L}\right)^2$	$\lambda_T = L\sqrt{\kappa\frac{GJ}{EI_\omega}}$	$\kappa=\frac{W_C}{\Im_C}=1-\frac{J}{\Im_C}$
FLEXURE I	$\begin{bmatrix} 0 & 0 & 0 & 0 \\ 0 & GA & -GA & 0 \\ 0 & -GA & GA+N_0 & 0 \\ 0 & 0 & 0 & EI_z \end{bmatrix}$	$K^2=0; K^2=\left(\frac{\lambda_N}{L}\right)^2$	$\lambda_N = L\sqrt{\kappa\frac{N_0}{EI_z}}$	$\kappa=\frac{GA}{GA+N_0}$
DISTORTION	$\begin{bmatrix} EI_b & 0 & 0 & 0 \\ 0 & GW_D & -GW_D & 0 \\ 0 & -GW_D & GW_D & 0 \\ 0 & 0 & 0 & EI_D \end{bmatrix}$	$K^2=2\left(\frac{\lambda_D}{L}\right)^2\left[\alpha_D\pm\sqrt{\alpha_D^2-1}\right]$	$\lambda_D = L\sqrt[4]{\frac{EI_b}{4EI_D}}$	$\alpha_D=\frac{\sqrt{EI_bEI_D}}{2GW_D}$
FLEXURE II	$\begin{bmatrix} k & 0 & 0 & 0 \\ 0 & GA & -GA & 0 \\ 0 & -GA & GA & 0 \\ 0 & 0 & 0 & EI_z \end{bmatrix}$	$K^2=2\left(\frac{\lambda_W}{L}\right)^2\left[\alpha_W\pm\sqrt{\alpha_W^2-1}\right]$	$\lambda_W = L\sqrt[4]{\frac{k}{4EI_z}}$	$\alpha_W=\frac{\sqrt{kEI_z}}{2GA}$

Table I. Generalised local stiffness, eigenvalues and associated slenderness at the four problems.

2. Generalised concept of slenderness of straight beams with constant cross-section

It can be shown that the slenderness associated to each problem is the main parameter governing the response of the beam. Nevertheless, we established its definition in every case in a direct manner by considering the *qualitative* definition $\lambda=KL$, but disregarding a general formula. On the other hand, typical values of α_D and α_W defined at table I are less than 1% and, being those equal to ε with $0\leq\varepsilon<<1$, we find out that:

$$K=\pm\frac{\lambda_D}{L}\left[\sqrt{1+\varepsilon}\pm i\sqrt{1-\varepsilon}\right] \tag{10}$$

And the parameter λ_D can be written into both the form:

$$\lambda_D=|\Re K|L-O(\varepsilon)=|\Im K|L+O(\varepsilon) \tag{11}$$

Where O(ε) is *the order of magnitude* of the rest of real and imaginary parts in the Bachmann-Landau notation, that can be evaluated by developing in a power series of ε the functions $\sqrt{1+\varepsilon}$ and $\sqrt{1-\varepsilon}$ respectively. This means that a real and positive number C exists so that $O(\varepsilon)<C\varepsilon$ .Consequently, if we assume that a phenomenon is considered as ***elementary*** when governed by ***one unique mechanical parameter***, then the eigenvalues that correspond to this problem can always be written in the form:

$$K=\Re K\pm i\Im K=A\{[1+O_1(\varepsilon)]\pm i[1-O_2(\varepsilon)]\} \tag{12}$$

Where A is a real number and $O_i(\varepsilon)$ follow the rules given to define $O(\varepsilon)$. We can thus define the slenderness associated to this elementary problem as:

$$\lambda=L\lim_{\varepsilon\to0}\sqrt{(\Re K cos\phi)^2+(\Im K sen\phi)^2}\ \text{, being}\ \phi=arctan\frac{\Im K}{\Re K} \tag{13}$$

It can be seen that this formula covers all the examples studied. In particular, when it is applied to the evaluation of λ_D and λ_W, the term ε is equal to the shear deformation factor.

3. Structural response and approximation to the problem of selecting a 1D model

Let us consider the solution of the elementary problems described at section 1 for one particular common case: torsion (flexure or distortion respectively) of a straight element simply supported, i.e. with rotations (transverse displacement or distortion respectively) blocked and free torsion warp (rotations or distortion warp respectively) at both ends, and subjected to a punctual torque (punctual force P or punctual bi-shear M_D respectively, this last derived from a torque) at the mid-span. Figure 1 represents the normalised values of the constitutive shear forces

and "bi-shears" characteristics of the four problems that have been analysed as functions of the slenderness. It can be seen that the bigger λ is the less the values are of all functions so we can conclude that in beams *sufficiently* slender (to establish a numerical value for such border is not within the scope of this paper) the structural behaviour is simpler. The responses then become pure torsion of Saint-Venant or without distortion in the case of torsion actions and cable response in the case of bending action. Those remarks authorise a structural simulation which is simpler. The other end of the range of variation of the slenderness, i.e. λ=0, conduces to 4 solutions with identical structure to the flexure of Timoshenko (two generalised displacements and K=0).

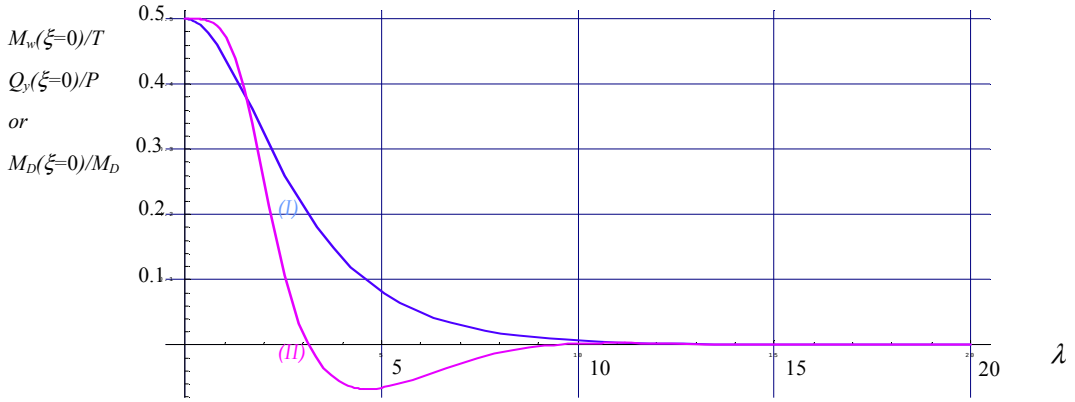

Figure 1. Distribution of (I) Warped part of torsion moments-Constitutive part of shear efforts of the beam-column and (II) Bi-shears of distortion-shear efforts of the floating beam, normalised, evaluated at ξ=0 and as function of the slenderness λ.

4. Revision of analogies in the problems of beams

Finally, let us consider the analogies at the problems relative to the beam. Table II compares the four elementary responses described at the section 1: general mixed torsion, the beam-column, the distortion and the floating beam. The first pair of problems presented are analogous as are the second pair. The organisation of the table respects this fact and establishes the equivalences in terms of displacements, forces, stiffness and loads. It is noted that all the elementary responses incorporate herein the shear deformation.

	components of E(ξ)				**coefficients de D**			**loads Q(ξ)**	
Ia.torsion	θ_x	φ	M_x	$B_{\dot{\omega}}$	GW_C	$EI_{\dot{\omega}}$	$G\Im_C$	m_x	$b_{\dot{\omega}}$
Ib.flexure	v	θ_z	Q_y	M_z	GA	EI_z	$GA+N_0$	q_y	m_z
IIa.distortion	γ_D	φ_D	M_D	B_D	GW_D	EI_D	EI_b	m_D	b_D
IIb.flexure	v	θ_z	Q_y	M_z	GA	EI_z	k	q_y	m_z

Table II. First level of analogies between the problems relative to the beam

We can state that the analogy is absolute between the problems of torsion and the beam column (when subjected to tension forces) or between the problems of distortion and the beam of Winkler, even in the case that we consider the deformations due to shear. The equations that govern the torsion problem are nevertheless slightly different than the ones of distortion.

When we consider that the torsion module J, the axial force N_0, the frame stiffness EI_b and the ballast coefficient k are null (always when the generalised slenderness approaches to 0), the above are reduced to three identical problems that incorporate systematically the deformations due to shear. This is the Second level of analogy for all responses of the beam.

Finally, when the shear deformations are excluded, the resultant equivalences are between the pure warped torsion ($\varphi = \theta_x'$), the flexure of Navier ($\theta_z = v'$) and the distortion without shear deformation ($\varphi_D = \gamma_D'$). From a

practical point of view, the most interesting analogy is the second level one: it conduces easily to analytical solutions for the torsion and distortion problems starting from the well-known ones of flexure.

	components of E(ξ)				coefficients of D		loads Q(ξ)	
torsion	θ_x	φ	M_x	$B_{\hat{\omega}}$	GW_C	$EI_{\hat{\omega}}$	m_x	b_ω
flexure	v	θ_z	Q_y	M_z	GA	EI_z	q_y	m_z
distortion	γ_D	φ_D	M_D	B_D	GW_D	EI_D	m_D	b_D

Table III. Second level of analogies between the problems relative to the beam

Nevertheless, from a more conceptual or theoretical point of view, we shall give weight to the concept of slenderness as the main parameter incorporated to and governing the response of the beam and its simulation.

References

[1] Benscoter, S.U., *"A theory of torsion bending for multicell beams"*, Journal of Applied Mechanics, March 1954, pp. 25-34 (1954)

[2] Brush, D.O. y Almroth, B.O., *"Buckling of bars, plates and shells"*, McGraw-Hill (1975)

[3] Dabrowski, R., *"Influence of shear deformation on warping torsion of box girders with deformable profiles having flexural stiffness"*, Der Buaingenieur, November 1965, pp.444-449 (1965)

[4] Hetenyi, M., *"Beams on elastic foundation"*, The University of Michigan Press (1946)

[5] Kollbrunner, C.F. y Basler, K., *"Torsion in structures. An engineering approach"*, Springer (1969)

[6] Krístek, V., *"Theory of box girders"*, Wiley (1979)

[7] Manterola, J., *"La sección abierta y cerrada bajo solicitación excéntrica"*, Puentes II, monografía Nº **15** de la A.F.C.E. (1976)

[8] Maisel, B.I. y Roll, F., *"Methods of analysis and design of concrete box beams with side cantilevers"*, C.& C.A. Technical report **42**.494 (1974)

[9] Monleón, S., *"Ingeniería de puentes: análisis estructural"*, S.P.U.P.V., Ref. 97.067 (1997)

[10] Monleón, S., *"Tópicos del análisis unidimensional de estructuras. Parte 2. Placas y láminas"*, Revista Internacional de Métodos Numéricos para Cálculo y Diseño en Ingeniería. Vol. 11, **1**, 37-59 (1995)

[11] Monleón, S., *"Análisis de vigas, arcos, placas y láminas: una presentación unificada"*, 2ª Ed., Editorial U.P.V., Ref. 2001.4122 (2001)

[12] Oden, J.T. y Ripperger, E.A., *"Mechanics of elastic structures"*, Mc Graw-Hill, 2ª Ed. (1981)

[13] Oumanski, A.A., *"Torsion et fléxion des constructions aéronautiques en voiles minces"*, Oborongiz (1939)

[14] Saint-Venant, B. de, *"De la torsion des prismes"*, Tome XIV de l´Académie des Sciences, Paris (1855)

[15] Vlassov, B.Z., *"Pièces longues en voiles minces"*, Eyrolles Editeurs, 2ª Ed. (1962)

Proceedings of the 6th International Conference on
Computation of Shell and Spatial Structures
IASS-IACM 2008: "Spanning Nano to Mega"
28-31 May 2008, Cornell University, Ithaca, NY, USA
John F. ABEL and J. Robert COOKE (eds.)

Element-free solution of geometrically exact rod elastostatics based on intrinsic (material) field variables

Carlos LÁZARO*, Salvador MONLEÓN, Alberto DOMINGO

*Departamento de Mecánica de Medios Continuos y Teoría de Estructuras
ETS Ingenieros de Caminos, Canales y Puertos
Universidad Politécnica de Valencia
Camino de Vera s/n, 46022 Valencia, Spain
carlafer@mes.upv.es

Abstract

Among the one–dimensional models available for non linear analysis of rods, the one proposed by Simó [5] as a extension of the work of Reissner and Antman is capable to treat arbitrarily large rotations of the cross–sections, and is thus called *geometrically exact rod model*. Several general–purpose finite element solutions based on different parmetrizations have been proposed (Simó and Vu-Quoc [6], Ibrahimbegović [2], Jelenić and Crisfield [3] and others). In such solutions the field variables need to be referred to the general spatial frame in order to carry the assembly of the element equations (variables are then said to be expressed in the spatial form). In contrast to this situation, the constitutive equations and the equilibrium equations of the problem are most naturally expressed using intrinsic variables (the material form of the variables). Starting from the late facts, the material form of the variational principles is deduced and element-free solutions based on these principles are presented.

1 Introduction

The *geometrically exact rod model* was formulated by Simo [5] starting from the works of Reissner and Antman [1]. It allows for a exact kinematic description of finite rotations and displacements and has been extensively studied by several authors. Most general-purpose finite element formulations of the model are based on the spatial form of the field variables. This spatial formulation allows for a direct assembly of the element tangent stiffness matrix into the global stiffness, which is very convenient. Although the spatial form of the tangent operator is very concise (if the natural parametrization of rotations is used), it is based on the spatial form of the element constitutive matrix, which has to be evaluated in each integration point by means of transformations of its blocks through the Gauss point rotations, which is a costly operation. Another drawback of the spatial formulation is the need of transforming the section forces to the section reference frame after each increment if such information is needed. In this work we examine the formulation of the model variables and solutions in terms of the intrinsic (material) field variables.

2 Kinematics, deformation variations and field equations

In the following we use Simo's terminology and notation. Intrinsic –also called material– variables (denoted by capital letters) are referred to the section reference frame. Spatial variables (denoted by small

letters) are referred to the fixed frame. Cross–sections of the rod are assumed to undergo a rigid body motion, translating and rotating during the deformation process. The position vector of a material point can be written in terms of its relative location into the section $\boldsymbol{r}^*$, and the position of the centroid of the section $\boldsymbol{x}$ as $\boldsymbol{x}^* = \boldsymbol{x} + \boldsymbol{r}^*$ and $\boldsymbol{r}^* = \boldsymbol{\Lambda}_{\rm d}\,\boldsymbol{\Lambda}_0\,\boldsymbol{R}^* = \boldsymbol{\Lambda}\,\boldsymbol{R}^*$. Section points rotate from a reference (material) configuration (described by $\boldsymbol{R}^*$) to the initial configuration through $\boldsymbol{\Lambda}_0$, and then to a deformed (actual) configuration through $\boldsymbol{\Lambda}_{\rm d}$. Composition of both rotations produces the rotation tensor $\boldsymbol{\Lambda}$, which together with $\boldsymbol{x}$ are the **configuration functions** of the model. The 1D deformation gradient $\partial \boldsymbol{x}^*/\partial S$ can be written as $\boldsymbol{\Gamma} + \boldsymbol{K} \times \boldsymbol{R}^*$, where $\boldsymbol{\Gamma} = \boldsymbol{\Lambda}^{\mathsf{T}}\boldsymbol{x}^{'}$ (elongation and shear) and $\widehat{\mathbf{K}} = \boldsymbol{\Lambda}^{\mathsf{T}}\boldsymbol{\Lambda}^{'}$ (change of orientation) are the **intrinsic generalized deformations**. The material configuration variations are $\delta\boldsymbol{\chi} = \boldsymbol{\Lambda}^{\mathsf{T}}\,\delta\boldsymbol{x}$ and $\delta\widehat{\boldsymbol{\Omega}} = \boldsymbol{\Lambda}^{\mathsf{T}}\delta\boldsymbol{\Lambda}$ (the last one is called *spin*). Let's introduce the variations $\delta\boldsymbol{\Gamma}$ and $\delta\boldsymbol{K}$ as conjugate variables to the section forces and moments $\boldsymbol{N}$, $\boldsymbol{M}$. Then, the intrinsic form of the **virtual work equation** (with $\boldsymbol{K}$ and $\delta\boldsymbol{\Omega}$ as axial vectors of the change of orientation and the spin)

$$\int_{\Gamma}(\boldsymbol{N}\cdot\delta\boldsymbol{\Gamma} + \boldsymbol{M}\cdot\delta\boldsymbol{K})\,dS = \int_{\Gamma}(\boldsymbol{Q}_n\cdot\delta\boldsymbol{\chi} + \boldsymbol{Q}_m\cdot\delta\boldsymbol{\Omega})\,dS + \boldsymbol{N}_1\cdot\delta\boldsymbol{\chi}(S_1) + \boldsymbol{N}_2\cdot\delta\boldsymbol{\chi}(S_2) + \boldsymbol{M}_1\cdot\delta\boldsymbol{\Omega}(S_1) + \boldsymbol{M}_2\cdot\delta\boldsymbol{\Omega}(S_2), \quad (1)$$

holds for every admissible variation $(\delta\boldsymbol{\chi}, \delta\boldsymbol{\Omega})$ iff $(\boldsymbol{x}, \boldsymbol{\Lambda})$ is an equilibrium configuration. It can be shown from the geometry of the configuration space, that the deformation variations can be expressed as functions of the configuration: $\delta\boldsymbol{\Gamma} = (\delta\boldsymbol{\chi})^{'} + \boldsymbol{K}\times\delta\boldsymbol{\chi} + \boldsymbol{\Gamma}\times\delta\boldsymbol{\Omega}$, and $\delta\boldsymbol{K} = (\delta\boldsymbol{\Omega})^{'} + \boldsymbol{K}\times\delta\boldsymbol{\Omega}$. Integration by parts leads to the **equilibrium equations** $\boldsymbol{N}^{'} + \boldsymbol{K}\times\boldsymbol{N} + \boldsymbol{Q}_n = \boldsymbol{0}$, and $\boldsymbol{M}^{'} + \boldsymbol{K}\times\boldsymbol{M} + \boldsymbol{\Gamma}\times\boldsymbol{N} + \boldsymbol{Q}_m = \boldsymbol{0}$. **Consitutitve equations** are naturally established between intrinsic variables.

3 Consistent tangent operator

The consistent linearization of the internal virtual work requires the evaluation of the **second variations** of the configuration, which, using the geometrical properties of the configuration space, lead to the following expressions: $\Delta(\delta\boldsymbol{\chi}) = -\Delta\boldsymbol{\Omega}\times\delta\boldsymbol{\chi}$, $\Delta(\delta\boldsymbol{\Omega}) = \boldsymbol{0}$, $\Delta(\delta\boldsymbol{\chi}^{'}) = -\Delta\boldsymbol{\Omega}^{'}\times\delta\boldsymbol{\chi} - \Delta\boldsymbol{\Omega}\times\delta\boldsymbol{\chi}^{'}$, $\Delta(\delta\boldsymbol{\Omega}^{'}) = \boldsymbol{0}$. The linearizaton of the internal virtual work equation leads to the **geometrical** tangent **operator**,

$$\begin{bmatrix} \mathbf{0} & \widehat{\mathbf{K}}\widehat{\mathbf{N}} & \mathbf{0} & \mathbf{0} \\ \widehat{\mathbf{N}}\widehat{\mathbf{K}} & \widehat{\mathbf{N}}\widehat{\mathbf{\Gamma}}+\widehat{\mathbf{M}}\widehat{\mathbf{K}} & \widehat{\mathbf{N}} & \widehat{\mathbf{M}} \\ \mathbf{0} & -\widehat{\mathbf{N}} & \mathbf{0} & \mathbf{0} \\ \mathbf{0} & \mathbf{0} & \mathbf{0} & \mathbf{0} \end{bmatrix}, \quad (2)$$

and to the **constitutive operator**

$$\begin{bmatrix} -\widehat{\mathbf{K}}\mathbf{C}_{\Gamma\Gamma}\widehat{\mathbf{K}} & -\widehat{\mathbf{K}}\,(\mathbf{C}_{\Gamma\Gamma}\widehat{\mathbf{\Gamma}}+\mathbf{C}_{\Gamma K}\widehat{\mathbf{K}}) & -\widehat{\mathbf{K}}\mathbf{C}_{\Gamma\Gamma} & -\widehat{\mathbf{K}}\mathbf{C}_{\Gamma K} \\ -(\widehat{\mathbf{\Gamma}}\mathbf{C}_{\Gamma\Gamma}+\widehat{\mathbf{K}}\mathbf{C}_{K\Gamma})\,\widehat{\mathbf{K}} & -(\widehat{\mathbf{\Gamma}}\mathbf{C}_{\Gamma\Gamma}+\widehat{\mathbf{K}}\mathbf{C}_{K\Gamma})\,\widehat{\mathbf{\Gamma}}-(\widehat{\mathbf{\Gamma}}\mathbf{C}_{\Gamma K}+\widehat{\mathbf{K}}\mathbf{C}_{KK})\,\widehat{\mathbf{K}} & -(\widehat{\mathbf{\Gamma}}\mathbf{C}_{\Gamma\Gamma}+\widehat{\mathbf{K}}\mathbf{C}_{K\Gamma}) & -(\widehat{\mathbf{\Gamma}}\,\mathbf{C}_{\Gamma K}+\widehat{\mathbf{K}}\mathbf{C}_{KK}) \\ \mathbf{C}_{\Gamma\Gamma}\widehat{\mathbf{K}} & \mathbf{C}_{\Gamma\Gamma}\widehat{\mathbf{\Gamma}}+\mathbf{C}_{\Gamma K}\widehat{\mathbf{K}} & \mathbf{C}_{\Gamma\Gamma} & \mathbf{C}_{\Gamma K} \\ \mathbf{C}_{K\Gamma}\widehat{\mathbf{K}} & \mathbf{C}_{K\Gamma}\widehat{\mathbf{\Gamma}}+\mathbf{C}_{KK}\widehat{\mathbf{K}} & \mathbf{C}_{K\Gamma} & \mathbf{C}_{KK} \end{bmatrix}. \quad (3)$$

The virtual work equation can be linearized as $\Delta\,(\delta W_{int} - \delta W_{ext})$. If the configuration $\boldsymbol{x}, \boldsymbol{\Lambda}$ is an equilibrium configuration for a given load factor λ, then the virtual work is zero for every admissible variation, and $\Delta\delta W_{int} = \Delta\delta W_{ext}$. This expression defines the tangent equilibrium of the geometrically exact model.

4 Numerical experiments

In order to check the performance of the operator we fisrt consider the linear problem consistently derived from the general nonlinear case. For this purpose the generalized deformations may be split into initial and deformational parts in the following manner $\boldsymbol{\Gamma} = \boldsymbol{\Gamma}_0 + \boldsymbol{\Gamma}_{\rm d}$, $\boldsymbol{K} = \boldsymbol{K}_0 + \boldsymbol{K}_{\rm d}$. In the linear problem, *equilibrium is established in the undeformed configuration*, thus only the initial parts of the deformations appear in the equations. The linear equations are $\boldsymbol{N}^{'} + \boldsymbol{K}_0\times\boldsymbol{N} + \boldsymbol{Q}_n = \boldsymbol{0}$ and $\boldsymbol{M}^{'} + \boldsymbol{K}_0\times\boldsymbol{M} + \boldsymbol{\Gamma}_0\times\boldsymbol{N} + \boldsymbol{Q}_m = \boldsymbol{0}$, with $\boldsymbol{\Gamma}_0 = \{1, 0, 0\}$ and $\boldsymbol{K}_0 = \{\tau_0, 0, \kappa_0\}$ (torsion and curvature of the undeformed rod centerline). The initial deformations are not subject to variation, thus only the constitutive part of the tangent operator is derived.

We search numerical solutions using the *Point Interpolation Method* (PIM), Liu [4]. For this purpose N *field nodes* are scattered along the problem domain (the interval $[S_1, S_2]$) in such a way that intervals with high nodal density correspond to high values of curvature and/or torsion. The domain is divided into a certain number of integration cells N_{cells}. For convenience, cell ends are chosen to be coincident with field nodes (although they don't need to). The *support domain* of each cell is defined as an interval with the same center as the integration cell, and radius d_s; the radius is iteratively determined as the minimum value for which the relation between d_s and the support domain nodal average spacing is greater than a pre–determined parameter α_s (typically between 1.0 and 6.0). The number of nodes belonging to the support domain n_s is equal or greater than the number of those belonging to the integration cell. A number of n_s PIM shape functions are constructed using the n_s support domain nodes for each integration cell — this procedure is thoroughly explained in Liu [4]. Integration is carried on by means of a gaussian quadrature; the number of quadrature points in a cell n_g is chosen so that the polynomial shape functions are exactly integrated ($n_g \geq n_s/2$). Shape functions and their derivatives are implemented into the virtual work equation. The solution vector contains the nodal intrinsic configuration increments $\Delta\boldsymbol{\Phi} = \{\Delta\boldsymbol{\chi}, \Delta\boldsymbol{\Omega}\}$, which need to be transformed into spatial form in order to understand them as displacements and rotations referred to the fixed frame $\Delta\boldsymbol{x} = \boldsymbol{\Lambda}_0\,\Delta\boldsymbol{\chi}$ and $\Delta\boldsymbol{\omega} = \boldsymbol{\Lambda}_0\,\Delta\boldsymbol{\Omega}$. Furthermore, it is convenient to work with incremental rotations $\Delta\boldsymbol{\theta}$, which are related to $\Delta\boldsymbol{\omega}$ through $\mathbf{T}(\boldsymbol{\theta})$ (Ibrahimbegović *et al.* [2]). In linear problems it can be shown that $\mathbf{T}(\boldsymbol{\theta}) = \mathbf{1}$, therefore $\Delta\boldsymbol{\theta} = \boldsymbol{\Lambda}_0\,\Delta\boldsymbol{\Omega}$.

A simply supported straight beam with flexural rigidity $EI = 2.5\ 10^2$, shear stiffness $GA = 1.0\ 10^5$, section height $h = 0.1$ and length $L = 10$, under a uniform load $q = 1.0$ is considered. Element–free implementation behavior is tested under different conditions: (a) increasing number of field nodes, ranging from $N = 3$ to $N = 25$, (b) increasing support domain normalized radius, ranging from $\alpha_s = 1.1$ to $\alpha_s = 11.1$; this is equivalent to increasing order of the interpolation polynomials, and (c) varying size of integration cells, ranging from 2– to 7–node cells (1 to 6 intervals). A sensitivity analysis is made for every size of the integration cells. The following deflection–related error parameter is considered for tracing convergence (Liu [4]):

$$err = \frac{\sqrt{\int_0^L (v_{num} - v_{exact})^2\ dS}}{\sqrt{\int_0^L v_{exact}^2\ dS}}. \tag{4}$$

Results show for a given size of the integration cell and for fixed α_s a slow decay of the error parameter with increasing number of field nodes N. If the node number is fixed, the error parameter falls remarkably when the support domain normalized radius α_s reaches a certain value. This value is rather independent of the number of nodes. For 2–node integration cells and $\alpha_s = 4.1$ (interpolation polynomials of order 7, $n_g = 4$), $\log_{10}(err)$ falls under -7. For 3–node integration cells values of $\log_{10}(err)$ under -10 are achieved with $\alpha_s = 3.1$ (interpolation polynomials of order 6, $n_g = 3$). Remarkably, increasing the support domain radius above these values does not lead to lower errors.

In order to reach the same accuracy ($\log_{10}(err)$ under -10), 2–node integration cells need $\alpha_s = 6.1$ (interpolation polynomials of order 11, $n_g = 6$). 4–node cells show, with increasing number of field nodes, a rather unstable behavior for values of α_s under 6.1; interpolation polynomials of order 13 ($\alpha_s = 7.1$, $n_g = 7$) are required to reach high accuracies. 5–node cells show good results with $\alpha_s = 4.1$, and 7–node cells need again $\alpha_s = 7.1$.

Two parameters are directly related to the computational efficiency of the solution: the number of field nodes N and the total number of Gauss points N_g. Focusing our attention on the stable solutions for increasing N, the better choices for different integration cell sizes are shown in the following table. Results show very good convergence properties of mesh–free solutions with a low number of field nodes, 3–node integration cells and interpolation polynomials of order 6. For this case the total number of Gauss points is $N_g = 4N_{cells} - 2$, which is always greater than the number of field nodes $N = 2N_{cells} + 1$. The intrinsic formulation operates with no need of coordinate transformation of the constitutive matrix. Thus, it is very convenient from the computational viewpoint when the number of Gauss points is greater than the number of field nodes, as in the proposed interpolation.

	2–node cell	3–node cell	5–node cell
N_{cells}	12	3	2
N	13	7	9
N_g	60	10	8
α_s (order)	6.1 (7)	3.1 (6)	4.1 (8)

Table 1: Lowest number of field nodes and gauss points necessary to reach high accuracies

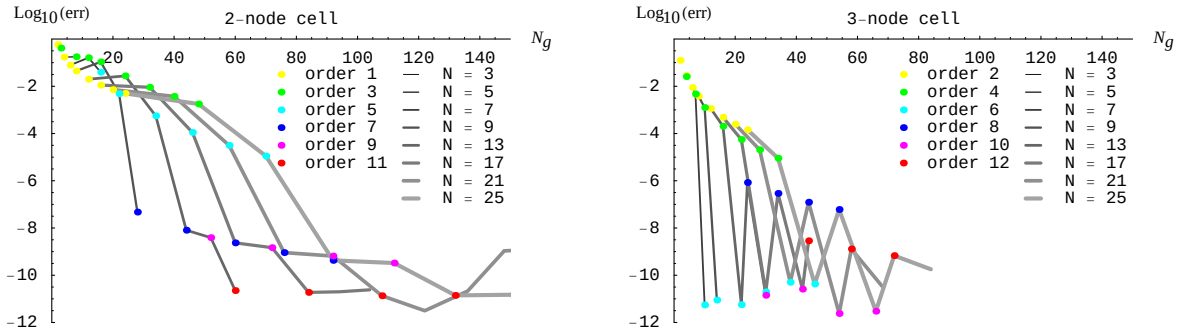

Figure 1: Convergence of the element–free solution

5 Conclusions

In this work, a novel form of the tangent operator for the geometrically exact beam model has been proposed. Geometrical and constitutive parts of the operator are deduced using the geometrical properties of the configuration space. Incremental–iterative solutions can be developed from the tangent operator. The linear version of this procedure has been developed and implemented by means of an element–free method (Point Interpolation Method), which is especially well suited to the 1D problem. In a next stage, nonlinear incremental (–iterative) solutions are being implemented on the basis of the tangent operator introduced in section 3. Economy in the iterative process may be achieved due to the properties of the intrinsic solution.

References

[1] Antman S.S., Nonlinear Problems of Elasticity (2nd edn), Applied Mathematical Sciences, Springer, 2005.

[2] Ibrahimbegović A, Frey F, Kozar I. Computational aspects of vector–like parametrization of three–dimensional finite rotations, *International Journal for Numerical Methods in Engineering* 1995; **38**: 3653–3673.

[3] Jelenić G., Crisfield M.A., Geometrically exact 3D beam theory: implementation of a strain–invariant finite element for statics and dynamics, *Computer Methods in Applied Mechanics and Engineering* 1999; **171**: 141–171.

[4] Liu G.R., Mesh Free Methods, CRC Press, 2003.

[5] Simo J.C., A finite strain beam formulation. The three–dimensional dynamic problem. Part I, *Computer Methods in Applied Mechanics and Engineering* 1985; **49**: 55–70, North–Holland.

[6] Simo JC, Vu-Quoc L. A three–dimensional finite–strain rod model. Part II: Computational aspects, *Computer Methods in Applied Mechanics and Engineering* 1986; **58**: 79–116, North–Holland.

Proceedings of the 6th International Conference on
Computation of Shell and Spatial Structures
IASS-IACM 2008: "Spanning Nano to Mega"
28-31 May 2008, Cornell University, Ithaca, NY, USA
John F. ABEL and J. Robert COOKE (eds.)

Adding local rotational degrees of freedom to ANC beams

Ignacio Romero*, Juan J. Arribas

*E.T.S.I. Industriales, Universidad Politécnica de Madrid
José Gutiérrez Abascal, 2; 28006 Madrid; Spain
ignacio.romero@upm.es

Abstract

This work shows a simple finite element formulation that enables to impose concentrated moments and rotations to ANC beams which are finite elements that lack rotational degrees of freedom. The idea is based on an specific constraint that expresses in a simple form the relation between the deformation of the beam and the rotation of any of its sections. By controlling this sectional rotation, moments and angles can be easily imposed on any model.

1 Introduction

Finite element beam discretizations based on the Absolute Nodal Coordinate (ANC) Formulation have been recently proposed by Shabana and coworkers [1, 2]. Their greatest advantage over conventional beam models is that these new finite elements avoid the use of rotational degrees of freedom by using an elaborated set of nodal parameters. As a result, their implementation is straightforward, the mass matrix is constant, and they can employ arbitrarily complex material constitutive laws. Moreover, since no special nodal rotation updates are required, ANC beams can be incorporated into existing finite element codes with relative ease. We refer to Romero [3] for a recent comprehensive review.

The absence of rotational degrees of freedom is a great advantage, but it carries some undesirable consequences. From the point of view of nonlinear structural engineering, maybe the most important one is that neither concentrated moments nor rotations can be directly imposed to an ANC beam. These boundary conditions are extremely common in engineering analysis, and unless a simple way to impose them is devised, the use of ANC beams can not be widespread.

In this work we will show how to incorporate rotational degrees of freedom at those points where the boundary conditions are required, and how to link these degrees of freedom to those of the ANC section. From the mathematical standpoint this will amount to imposing that the "rotational part" of the section deformation equals the imposed rotation. How to clearly identify this "rotational part" is the goal of Section 2. From the numerical point of view, we will accomplish this goal by devising a discrete finite element that will transfer the rotational degrees of freedom to the section. To do so, the element must manage to convert the virtual work in the rotational degrees of freedom to virtual work in the ANC node.

2 ANC beams

Beams based on the absolute nodal coordinate formulation (ANC) were originally introduced in Shabana and Yacoub [1, 2] and have been analyzed an improved by Shabana and co-workers (see for example, [4, 5]). The main novelty of

the formulation is the deformation parametrization which, for each element e of the beam is of the form:

$$\boldsymbol{\varphi}_e(x,y,z,t) = \boldsymbol{S}_e(x,y,z) \begin{Bmatrix} \boldsymbol{a}_e(t) \\ \boldsymbol{b}_e(t) \\ \boldsymbol{c}_e(t) \end{Bmatrix} . \tag{1}$$

The matrix $\boldsymbol{S}_e$ contains the element interpolation functions and must be of the form:

$$\boldsymbol{S}_e(x,y,z) = \begin{bmatrix} \boldsymbol{J}_N(x,y,z) & \boldsymbol{0}_N & \boldsymbol{0}_N \\ \boldsymbol{0}_N & \boldsymbol{J}_N(x,y,z) & \boldsymbol{0}_N \\ \boldsymbol{0}_N & \boldsymbol{0}_N & \boldsymbol{J}_N(x,y,z) \end{bmatrix} , \tag{2}$$

where $\boldsymbol{0}_N$ is the N-dimensional zero row vector and $\boldsymbol{J}_N$ is an interpolation row vector of the form:

$$\boldsymbol{J}_N(x,y,z) = \langle 1,\ x,\ y,\ z,\ xy,\ xz,\ x^2,\ x^3\ \ldots x^{N-5} \rangle . \tag{3}$$

The constant N determines the degree of polynomial interpolation in the x direction and must be greater or equal to 7. For the rest of the article, as in the original work of Shabana and Yacoub [1, 2], we assume that $N = 8$, effectively setting the order of interpolation in the x direction to 3. In view of equation 1, the number of degrees of freedom per element is $3 \times N$, which for our choice equals 24.

The vector $\langle \boldsymbol{a}_e(t),\ \boldsymbol{b}_e(t),\ \boldsymbol{c}_e(t) \rangle^T$ contains the coefficients of the element interpolation functions, and can be associated with nodal degrees of freedom in the following way. Let $\boldsymbol{H}_e^\alpha$, for $\alpha = 1, 2$, be the set of 12 variables associated with the local node α belonging to element e:

$$\boldsymbol{H}_e^\alpha(t) = \left\langle \boldsymbol{\varphi}(\boldsymbol{X}_e^\alpha, t),\ \frac{\partial \boldsymbol{\varphi}(\boldsymbol{X}_e^\alpha, t)}{\partial x},\ \frac{\partial \boldsymbol{\varphi}(\boldsymbol{X}_e^\alpha, t)}{\partial y},\ \frac{\partial \boldsymbol{\varphi}(\boldsymbol{X}_e^\alpha, t)}{\partial z} \right\rangle^T . \tag{4}$$

The first vector in $\boldsymbol{H}_e^\alpha$ is simply the nodal position of the local α-th node at time t, and the remaining vectors the three tangent vectors to the local coordinate curves x, y, and z at the deformed configuration.

It can be verified that for the interpolation chosen above, the deformation $\boldsymbol{\varphi}_e$ can also be written as:

$$\boldsymbol{\varphi}_e(x,y,z,t) = \boldsymbol{D}_e(x,y,z) \begin{Bmatrix} \boldsymbol{H}_e^1(t) \\ \boldsymbol{H}_e^2(t) \end{Bmatrix} , \tag{5}$$

for a new interpolation matrix $\boldsymbol{D}_e$ related to $\boldsymbol{S}_e$. Although completely equivalent to expression (1), this new interpolation has the advantage that the set of variables $\langle \boldsymbol{H}_e^1,\ \boldsymbol{H}_e^2 \rangle^T$ has a more clear geometrical meaning, which has been further explored in Sopanen [5]

Let us define $\boldsymbol{G} = [\boldsymbol{t}_1, \boldsymbol{t}_2, \boldsymbol{t}_3]$, the three tangent vectors of the deformed beam. This tensor is invertible and, by the polar decomposition theorem, can be expressed as the product $\boldsymbol{F} = \boldsymbol{R}\boldsymbol{U}$, where $\boldsymbol{R}$ is a rotation tensor, and $\boldsymbol{U}$ is a symmetric, positive definite tensor. Since the goal of this work is to control the rotational part of the beam deformation, this is equivalent to imposing the value of $\boldsymbol{G}$ to be equal to a given rotation, leaving $\boldsymbol{U}$ unmodified. In other words, the geometrical interpretation of the beam degrees of freedom and the polar decomposition theorem shows that by imposing $\boldsymbol{R}$ to be as desired, the whole section of the beam will rotated as wanted.

To formulate such constraint mathematically, let $\boldsymbol{\theta}$ be a rotation vector and let $\exp[\boldsymbol{\theta}]$ be its associated rotation tensor. Since we would like to control the rotation part of the motion $\boldsymbol{R}$ by imposing the rotation vector $\boldsymbol{\theta}$ only, it would suffice to impose the constraint $\boldsymbol{R} = \exp[\boldsymbol{\theta}]$. The problem is, however, that there is no close form expression from the rotational part $\boldsymbol{R}$ of a given vector $\boldsymbol{G}$, which has to be obtained by means of an algorithm. The following result shows an equivalent statement which can be used explicitly to impose the desired constraint:

Theorem 2.1 *Let $\boldsymbol{F}$ be a second order tensor with positive determinant. Then there exists a unique rotation vector $\boldsymbol{\theta} \in \mathbb{R}^3$ such that*

$$\operatorname{skew}\Big[\exp[-\hat{\boldsymbol{\theta}}]\boldsymbol{F} \Big] = \boldsymbol{0} . \tag{6}$$

Furthermore, $\exp[\boldsymbol{\theta}]$ is equal to $\boldsymbol{R}$, the rotation that appears in the polar decomposition of $\boldsymbol{F}$.

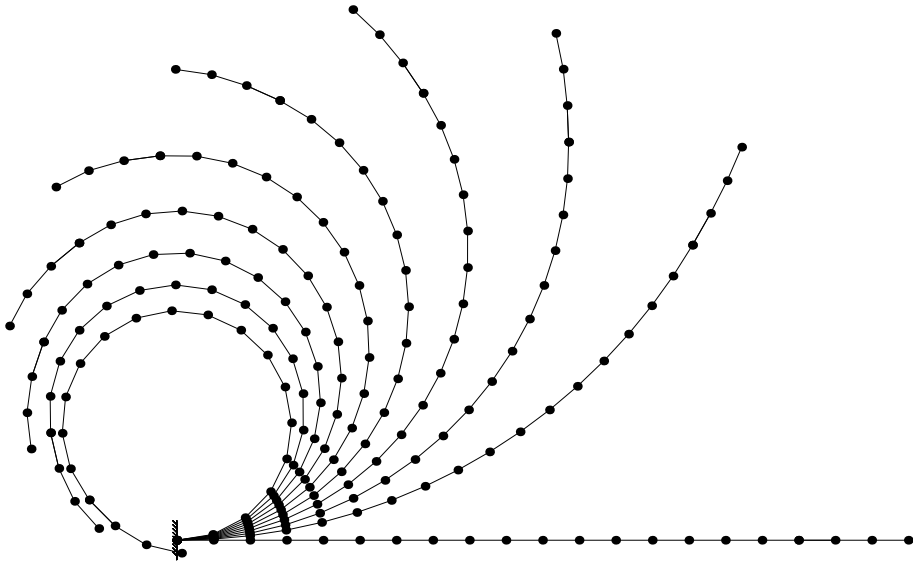

Figure 1: Deformation sequence of a cantilever beam under a concentrated moment at its tip.

In the previous equation we have employed the $\mathrm{skew}[]$ operator defined on second order tensors by $\mathrm{skew}[\boldsymbol{A}] = \frac{1}{2}(\boldsymbol{A} + \boldsymbol{A}^T)$. In other words, if we impose the constraint

$$\boldsymbol{g}(\boldsymbol{\theta}, \boldsymbol{G}) = \boldsymbol{0} \quad \text{with} \quad \boldsymbol{g}(\boldsymbol{\theta}, \boldsymbol{G}) = \mathrm{skew}\Big[\exp[-\hat{\boldsymbol{\theta}}(t)]\boldsymbol{G}(t)(\boldsymbol{G}^o)^{-1}\Big] , \tag{7}$$

then the rotation part of the section deformation $\boldsymbol{R}$ will be identical to the rotation $\exp[\boldsymbol{\theta}]$.

3 The finite element formulation

To implement the proposed constraint we assume that the beam equations result from the minimization of a potential energy $\Pi(\boldsymbol{\varphi})$. Then, using the classical penalty method, the constraint can be approximately imposed by minimizing the augmented potential energy

$$\Pi^\kappa(\boldsymbol{\varphi}, \boldsymbol{\theta}) = \Pi(\boldsymbol{\varphi}) + \Pi^g(\boldsymbol{\theta}, \boldsymbol{G}) , \qquad \Pi^g(\boldsymbol{\theta}, \boldsymbol{G}) = \frac{\kappa}{2} \left|\boldsymbol{g}(\boldsymbol{\theta}, \boldsymbol{G})\right|^2 , \tag{8}$$

where κ is a large positive number.

To obtain the equations of the internal forces resulting from this connecting element, the first variation of (8) should be calculated. The tangent stiffness is simply obtained by calculating the second variation of the same equation.

4 Numerical example

Imposing a simple torque on a ANC beam is a complex task as can be seen, for example, in Sopanen [5]. With the previous formulation, the task becomes trivial. To illustrate this, we use a the classical example of a cantilever beam of length $L = 1$, and bending stiffness $EI = 175000$. When a concentrated moment of modulus $M = 2\pi EI/L$ is applied at the beam's tip, it should bend 2π radians. In order to perform such simulation we simply add a new fictitious node at the beam's tip, a node that only has rotational degrees of freedom. After imposing the concentrated moment the beam bends as the figure 1. The errors at the tip are not due to the imposed moment, but rather related to the beam accuracy.

Acknowledgements

Financial support for this work has been provided by grant DPI2006-14104 from the Spanish Ministry of Education and Science.

References

[1] A. A. Shabana and R.Y. Yakoub. Three dimensional absolute nodal coordinate formulation for beam elements: theory. *ASME Journal of Mechanical Design*, 123(4):606–613, 2001.

[2] R.Y. Yacoub and A. A. Shabana. Three dimensional absolute nodal coordinate formulation for beam elements: implementation and applications. *ASME Journal of Mechanical Engineering*, 123(4):614–621, 2001.

[3] I. Romero. A comparison of finite elements for nonlinear beams: the absolute nodal coordinate and geometrically exact formulations. *Accepted for publication in Multibody System Dynamics*, 2008.

[4] J. Gerstmayr and A. A. Shabana. Efficient integration of the elastic forces and thin three-dimensional beam elements in the absolute nodal coordinate formulation. In J. M. Goicolea, J. Cuadrado, and J. C. García Orden, editors, *Multibody Dynamics 2005. ECCOMAS thematic conference*, Madrid, Spain, 21–24 June 2005.

[5] J. T. Sopanen and A. M. Mikkola. Description of elastic forces in absolute nodal coordinate formulation. *Nonlinear Dynamics*, 34:53–74, 2003.

Proceedings of the 6th International Conference on
Computation of Shell and Spatial Structures
IASS-IACM 2008: "Spanning Nano to Mega"
28-31 May 2008, Cornell University, Ithaca, NY, USA
John F. ABEL and J. Robert COOKE (eds.)

Finite element modeling of Kirchhoff rods

Juan VALVERDE, Francisco ARMERO*

* Structural Engineering, Mechanics and Materials
Department of Civil and Environmental Engineering
University of California, Berkeley, CA 94720, U.S.A.
email: armero@ce.berkeley.edu

Abstract

The traditional interest in rod and shell theories has been considerably revitalized in recent years by the availability of finite element methods able to resolve the most nonlinear and complex of these theories. A typical example of these considerations is the classical theory of Cosserat rods. However, most finite element formulations developed to date involve the case of shear deformable rods and beams, requiring in particular a C^0-continuous interpolation of the field variables only [1,2,3]. The consideration of rods incorporating the Kirchhoff assumption of no transverse shear strain (or, simply, Kirchhoff rods) is rare in these finite element treatments of Cosserat directed models. Nevertheless, this type of rods is of great technological and scientific importance in areas as diverse as astronautics, biology and smart composite materials, to name a few. The behaviour of DNA molecules is being the subject of a large amount of research. DNA molecules are composed by a double helix, each one being a thin biological filament. Some studies regarding the nature of this filaments [4,5] and the shaping of the helix from a straight filament as a mechanism for DNA formation [6] have been carried out using Kirchhoff rod models. Space tethers have attracted the interest in the astronautics community since late seventies. These space structures, which are composed by very long and thin rods (length to thickness ratios of the order $1/10^5$), are used to connect spacecrafts to satellites or other orbiting modules. This mechanical connection provides interesting capabilities [7], as the transfer of momentum between the orbiting bodies or the creation of electrical energy by means of an electricity conducting tether interacting with the geomagnetic field [8]. This situation motivates the development of reliable computational tools for the simulation of Kirchhoff rods leading to a complete understanding of their mechanical response.

We present in this contribution a formulation of Kirchhoff rods in the context of Cosserat theories and its finite element implementation. The proper parameterization of the basic variables characterizing the rotation of the cross-section (constrained in this case to be orthogonal to the rod's axis) is shown to be crucial in the development of the final formulation. In this context, a main challenge appears in the definition of a C^1-continuous finite element interpolation of the axis location in a curved configuration of the rod. A wide class of schemes is available in the literature for the interpolation of a general curve in space including, for example, formulations based on the classical Hermite polynomials. These issues apply even to the linear case, where the considered displacement interpolation needs to represent the basic rigid body modes without self-straining, as this basic invariance property is sometimes referred to, in a general curve representing the geometry of the reference axis of the rod.

We have considered different alternatives in this context and studied its adequacy for the mechanical problem at hand. In particular, we have identified a new C^1-continuous interpolation of the rod's kinematics that preserves the aforementioned invariance property. The new interpolation scheme is combined with mixed and enhanced treatments of the rod's strain to avoid the well-known membrane locking that appears in curved configurations

of the elements when trying to reproduce inextensional bending. Different numerical simulations illustrating the performance of the resulting finite elements will be presented.

References

[1] Simo JC. A finite strain beam formulation. Part I: The three-dimensional dynamic problem. *Computational Methods in Applied Mechanics and Engineering* 1985; **49**:55-70.

[2] Simo JC and Fox DD. On a stress resultant geometrically exact shell model. Part I: Formulation and optimal parametrization. *Computer Methods in Applied Mechanics and Engineering* 1989; **72**:267-304.

[3] Romero I and Armero F. An objective finite element approximation of the kinematics of geometrically exact rods and its use in the formulation of an energy-momentum conserving scheme in dynamics. *International Journal for Numerical Methods in Engineering* 2002; **54**:1683-1716.

[4] Manning RS, Maddocks JH and Kahn JD. A continuum rod model of sequence-dependent DNA structure. *Journal of Chemical Physics* 1996; **105**: 5626-5646.

[5] Goriely A and Tabor M. Nonlinear dynamics of filaments I. Dynamical instabilities. *Physica D* 1997; **105**: 20-44.

[6] Maiya BG and Ramasarma T. DNA, a molecular wire or not -- The debate continues. *Current Science* 2001; **80**(12): 1523-1530.

[7] Cosmo ML and Lorenzini EC. Tethers in Space Handbook (3rd edn). Smithsonian Astrophysical Observatory (NASA Marshall Space Flight Center), 1997.

[8] Valverde J, Escalona JL, Domínguez J and Champneys AR. Stability and bifurcation analysis of a spinning space tether. *Journal of Nonlinear Science* 2006; **16**(5): 507-542.